Rapid Communications

Discontinuity in the transport of strongly correlated two-dimensional hole systems in zero magnetic field

Jian Huang*
Department of Physics and Astronomy, Wayne State University, Detroit, Michigan 48201, USA

L. N. Pfeiffer and K. W. West
Department of Electrical Engineering, Princeton University, Princeton, New Jersey 08544, USA

(Received 15 November 2019; revised manuscript received 14 February 2020; accepted 17 March 2020; published 20 April 2020)

Adopting undoped ultraclean two-dimensional hole systems, we approach a strongly correlated limit by reducing the carrier density down to 1×10^9 cm^{-2}. The temperature dependence of the resistivity as a function of the carrier density reveals a characteristic energy scale displaying a benchmark critical behavior near a critical density of $p_c \sim 4 \times 10^9$ cm^{-2}. The insulating state below p_c exhibits a sharp resistance discontinuity in response to heating across a critical temperature $T_{c1} \sim 30$ mK, consistent with a first-order transition. The dc response also identifies a second critical temperature T_{c2} where linear IV behavior is recovered. Similar effects are also demonstrated by varying an external electric field. The results support a complex quantum phase transition with intermediate phases.

DOI: 10.1103/PhysRevB.101.161110

The behaviors of electrons in solids are profoundly influenced by electron-electron interaction. The strongly correlated regime draws special interest because the correlation can fundamentally modify the system by giving rise to remarkable many-body effects even to the point of driving quantum phase transitions (QPTs). Effects associated with such QPTs are fundamental to expanding frontiers in areas such as Wigner crystal (WC) [1], magnetism, nonconventional superconductivity, and topological matters. QPTs in two-dimensional (2D) systems are anticipated to be complicated because of the restricted quasi-long-range order and the associated symmetry breaking [2,3] that tend to drive a complex phase diagram. For example, a melting transition via a correlated intermediate phase has been predicted for the classical case [4–9]. Experimental results in the degenerate limit [10–19] have so far been insufficient for making identifications of clear signatures accompanying a phase transition, even though claims of a liquid-solid transition involving WCs were made [11,15,18,19]. This study focuses on the transport response in strongly correlated 2D systems in an ultralow disorder limit. Evidence of a phase transition is presented through both critical behaviors and sharp resistance discontinuities.

In correlated systems, effects stemming from disorders often complicate the situation through disorder localization [20]. Nevertheless, Anderson insulators differ from insulators caused by interaction (i.e., pinned WC cases). The interaction effect, reflected by $r_s = m^* e^2/\epsilon\hbar^2\sqrt{\pi p}$, becomes prominent only at low charge densities p. Taking the WC for example, the anticipated $r_s \geqslant 37$ [21] corresponds to ultradilute p, i.e., $\leqslant 5 \times 10^9$ cm^{-2} for GaAs 2D holes (or $\leqslant 8 \times 10^8$ cm^{-2} for electrons). The effective mass m^* is ~0.3-0.35 [22,23]. Localization easily occurs as the corresponding Fermi energy $E_F = n\pi\hbar^2/m^* \leqslant 30$ μeV falls below the typical disorder potential $eV_{\rm dis} \sim 0.1$ meV. e is the electron charge and ϵ is the dielectric constant. In addition, disorder screening is weakened because the large average charge spacing $2a$, where $a = 1/\sqrt{\pi p} \geqslant 100$ nm, becomes comparable to the screening length. As a result, the interaction effect is often overwhelmed. Experimental proof of such a disorder localization, i.e., in the insulating side of the 2D metal-to-insulator transition (MIT) [24], is the variable range hopping (VRH) transport [25,26] at finite temperatures T: $\sigma(T) = \sigma_0 \exp(-T^*/T)^{1/\gamma}$ ($\gamma = 2, 3$). T^* measures the difference to the mobility edge. The activated T dependence, however, is different from a phase transition in which discontinuity is anticipated [27].

The situation becomes more intriguing when disorder is further reduced and interaction is no longer a perturbation. Insulators other than the Anderson localization are found [28,29]. Previous experimental findings, i.e., in relation to thermal melting [11,15], mostly support a smooth transition or crossover without observing any singularity. Because the systems are often weak insulators [11] and the translational correlation length ξ is too small to support genuine long-range orders, the collective modes [18,19] alone are insufficient to clear up ambiguity associated with possible intermediate phases. Though the disorder effects are not yet well understood in this limit, they certainly contribute to reducing the long-range orders, as well as lowering the critical temperature (T_m) for a melting transition [9,27,30]. Therefore, accessing strongly correlated effects depends critically on the suppression of the disorders as suggested by recent studies [9,31].

Because doping is a major source of disorder in semiconductors, undoped 2D hole systems, in (100)

*jianhuang@wayne.edu

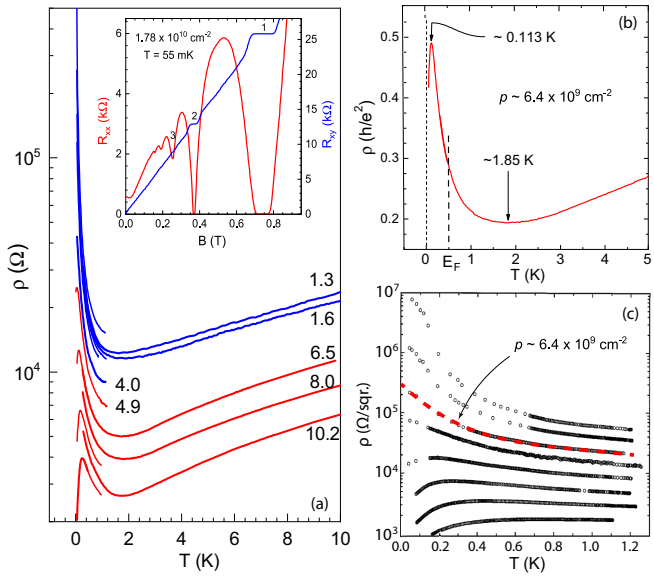

FIG. 1. T dependence of ρ for $p = 1.2$, 1.5, 1.8, 2.3, 2.8, 4.0, 4.9, 6.4, 9.5, and 12.5×10^9 cm^{-2}. Inset: Carrier density p is determined via the magnetoresistance and the Hall resistance. (b) $\rho(T)$ for $p = 6.4 \times 10^9$ cm^{-2}. (c) $\rho(T)$ taken from Ref. [15] showing insulating behavior for $p = 6.4 \times 10^9$ cm^{-2}.

GaAs/AlGaAs heterojunction-insulated-gate field-effect transistors (HIGFETs), are adopted for this study to reduce disorders down to the background level of the crystal growth chamber. At the heterointerface, accumulation of ultradilute 2D hole carriers down to $p = 6 \times 10^8$ cm^{-2} is realized [29,32] by solely biasing a top metal gate $d \sim 700$ nm above the 2D plane. With $d \gg a$, the reduction of r_s by dipolar screening [33] is minimized. The sample contains 6 mm $\times$ 0.8 mm Hall bars fabricated with a lithographic technique [34,35]. p at each fixed gate bias is determined by the quantum Hall measurement. The inset of Fig. 1(a) is for $p = 1.78 \times 10^{10}$ cm^{-2}.

The T dependence of the resistivity $\rho(T)$, measured with the four-probe ac lock-in technique, is shown in Fig. 1(a) for a number of p from 1.2 to 10.2×10^9 cm^{-2}. The current excitation is maintained $\leqslant 1$ nA to avoid heating. The measurement was carried out in both a dilution refrigerator and a helium-3 cryostat to cover a temperature range from $\sim$0.02 to $\sim$10 K. $\rho(T)$ reaches a local minimum ($T_{\rm min}$) that varies from 1.6 to 1.8 K for the range of p. $\rho(T)$ rises, or $d\rho/dT < 0$, below $T_{\rm min}$. Two different behaviors occur at lower T known as the signatures of the MIT: the delocalization effect renders a metal-like state, with $d\rho/dT > 0$, for p greater than a critical value $p_c \sim 4 \times 10^9$ cm^{-2}, while for $p < p_c$, ρ rises sharply with decreasing T.

We notice the p_c here is significantly lower than what is typically observed [15,36]. A comparison is drawn with a previous study of doped p-type GaAs 2D systems of similar heterostructures [15]. For $p = 6.4 \times 10^9$ cm^{-2} (or $r_s \sim 30$) in particular, an insulator was found and interpreted as a WC phase in Ref. [15] [dotted red line in Fig. 1(c)]. However, a metal state is observed here, as shown in Fig. 1(b), with ρ well below h/e^2. The reduction of disorder has clearly made the difference. We note that among nine different samples

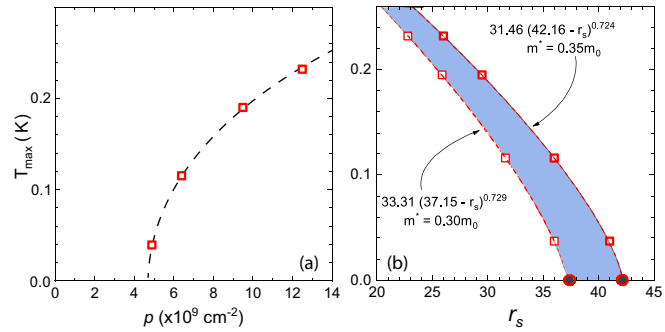

FIG. 2. (a) $T_{\rm max}$ vs p. The dotted line represents a nonlinear fit to $A \times (p - p_c)^B$. (d) The result in (b) replotted as a function of r_s, with m^* taken between $0.3m_0$ and $0.35m_0$.

(from different wafers) tested, there is only a slight variation in $p_c = (4.3 \pm 0.3) \times 10^9$ cm^{-2}.

As shown in Fig. 1(a), all metallic states start below a certain characteristic temperature, referred to as $T_{\rm max}$ since it is where $\rho(T)$ peaks, that varies with p. $T_{\rm max}$ is $\sim$113 mK for $p = 6.4 \times 10^9$ cm^{-2} as shown by Fig. 1(b). $T_{\rm max}$ as a function of p is plotted in Fig. 2(a). The dashed line is a nonlinear fit ($R^2 \approx 0.9997$) to $A \times (\frac{p-p_c}{p_c})^\alpha$ with fitting parameters $A = 187.62 \pm 4.2$ and the exponent $\alpha = 0.46 \pm 0.05$. The abrupt collapse of $T_{\rm max}$ at p_c of $(4.62 \pm 0.04) \times 10^9$ cm^{-2} represents a benchmark critical behavior. Figure 2(b) provides the corresponding r_s value, which is approximately 40.

Note that r_s depends on the m^*, which is not precisely known in the dilute limit due to the influences of the band mass (involving band mixing of light- and heavy-hole bands) and the spin-orbit coupling [37]. Here, we simply provide a range (shaded region) for $m^* = 0.3$-$0.35m_0$ which produces a critical r_s between 37 and 42. This range is moderately higher than the predicted onset point of the WC based on quantum Monte Carlo simulations [21] without considering the disorder effects.

The insulating behavior for $p < p_c$ is compared with Fig. 1(a) on double-logarithmic scales. Figure 3(a) shows the conductivity $\sigma(T) = 1/\rho(T)$ for $p = 1.2 \times 10^9$ cm^{-2} for T

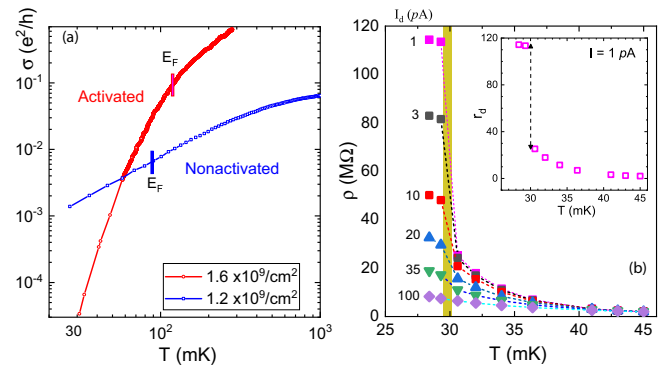

FIG. 3. (a) $\ln\sigma(T)$ vs $\ln T$ for $p = 1.2 \times 10^9$ cm^{-2} in comparison to an activated behavior for $p = 1.6 \times 10^9$ cm^{-2}. (b) $\rho(T)$ measured with different I_d. Dotted lines are a guide to the eye. The shaded region marks a sharp jump in ρ. Inset: discontinuity in the differential resistance r_d vs T.

from 1 K down to 30 mK. A nonactivated power-law T dependence [29] is observed for $T \leqslant 300$ mK. For comparison, an activated behavior found in a more disordered sample is also plotted—$\sigma(T)$ plummets exponentially by more than five orders of magnitude for the same T range. The ac signal excitation for this measurement is 0.5 nA. The influences due to the level of the current excitation have not been adequately addressed previously.

Despite the large $r_s \sim 60-70$, the nonactivated $\sigma(T)$ shown in Fig. 3(a) exhibit no clear features reflecting a phase transition. On the contrary, the resistance, ~500 kΩ at 30 mK, is low enough to support a strongly correlated liquid [29]. We first wondered whether this is related to the liquid reentrant behaviors at large r_s arising from the gate screening effect, which reduces the Coulomb interaction $e^2p^{1/2}$ to dipolar interaction $e^2d^2p^{3/2}$. However, this is ruled out by the below dc results because a discontinuity emerges in response to the change in signal excitation.

For $p \sim 3 \times 10^9$ cm^{-2}, ρ is measured at various T with a dc-IV technique. Adopting a femtoampere low noise source and an electrometer preamp with an input impedance of 10^{15} Ω, $\rho(T)$ is measured at various fixed current drives (I_d): 1, 3, 10, 20, 35, and 100 pA. As shown in Fig. 3(b), when $I_d =$ 100 pA is applied, $\rho(T)$ recovers the power law, consistent with the ac results. However, when $I_d = 35$ pA is used, a jump appears around 30 mK (shaded region), and it becomes increasingly stronger when less I_d is used.

For $I_d \leqslant 3$ pA, $\rho(T)$ becomes piecewise and a discontinuity appears via a jump of ~65 MΩ over less than 2 mK temperature change. The inset shows the differential resistance dV/dI as a function of T measured with 1 pA drive. Discontinuity in general is a signature of first-order phase transitions occurring across the phase boundaries. These insulating states are further examined with the dc measurement shown later. The location of the discontinuity is approximately $T \sim 30$ mK, which is referred to as the critical temperature T_{c1}. Current-induced heating is definitely ruled out because of the discontinuity. It is worth noting that below T_{c1} the resistance is extremely sensitive to the change in the drive up to 20 pA. The tiny current requirement, $\leqslant 3$ pA, for observing the discontinuity indicates that there is a critical excitation level above which the system is modified. Within the critical excitation, the T dependence at $T < T_{c1}$ is slight, ~1 MΩ per mK, compared to the discontinuity.

On the other hand, the $\rho(T)$ behavior above T_{c1} draws a contrast because the I_d dependence significantly weakens and is eventually washed out above 43 mK. The T dependence follows a general power law, distinct from the $T < T_{c1}$ scenario. $T = 43$ mK is referred to as T_{c2}. As shown below, T_{c2} actually marks a qualitative change in the dc-IV response.

Nonlinear dc-IV is performed for $p \sim 3 \times 10^9$ cm^{-2} at various T. The technique is well known for studying the pinned charge density waves (CDWs) [38]. Most previous studies with 2D semiconductor systems found weak insulators [11,15] in contrast to the pinned CDWs. Our dc-IV results are shown in Fig. 4. Figure 4(a) shows the dc-IV obtained below T_{c1}, at 28 mK, for $p \sim 3 \times 10^9$ cm^{-2}. The derivative shown in Fig. 4(b) captures an enormous subthreshold differential resistance dV/dI up to ~110 MΩ, comparable to that of

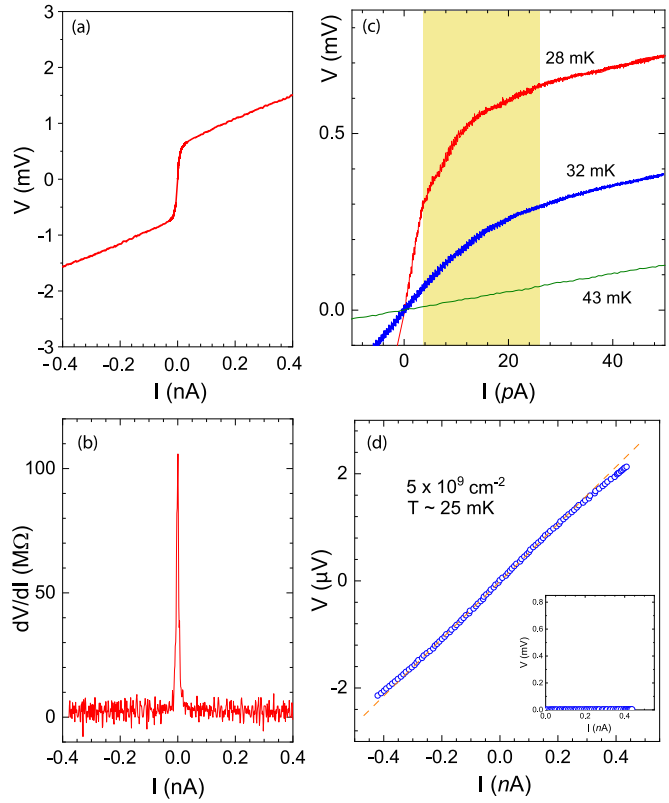

FIG. 4. (a) dc-IV measured for $p \sim 3 \times 10^9$ cm^{-2} (or $r_s \sim 50$), and (b) shows the derivative dV/dI. (c) Comparison of dc-IV behaviors obtained at $T = 28$, 32, and 43 mK. (d) dc-IV for $p > p_c$. Inset: the same plot on the same scales as (c).

pinned CDWs. The current corresponding to the threshold voltage $V_{\rm th} \sim 0.25$ mV is just ~2–3 pA. dV/dI plummets by two orders of magnitude when V exceeds $V_{\rm th}$.

The subthreshold resistance shown in Figs. 4(a) and 4(b) supports a transport response primarily in the form of potential energy because of the negligible current ($\leqslant 1$ pA). Because Anderson localization is excluded in our case, we consider the pinning scenario. Setting $eV_{\rm th}$ equal to the sum of all the single-particle potential energy $\epsilon = eV_{\rm th}/L$, the average particle displacement l (from the equilibrium) is found to be $\sim 0.13a$, where $a = 1/\sqrt{\pi p} \sim 100$ nm. $L \sim 1$ mm is the distance over which the electric field is applied. ϵ is approximately 3.5 neV, which is approximately 10^{-3} of k_BT_{c1} and 4×10^{-6} of the Coulomb energy E_c.

Because a true long-range order is prohibited in two dimensions [2], we consider quasi-long-range correlation length ξ. For the cases of charge pinning, ξ scales with dV/dI up to $V_{\rm th}$ and can be estimated at $V_{\rm th}$ by balancing the total potential energy $N\epsilon$ and the pinning energy $-(1/2)\kappa a$ [11,12]. $\kappa = 0.245e^2p^{3/2}/4\pi\epsilon_0\epsilon$ is the sheer modulus and $N = p\xi^2$ is the particle numbers within a single domain. Utilizing the average particle displacement l found earlier, N is estimated as $\sim 10^5$, which corresponds to $\xi \geqslant 50$ μm.

Figure 4(c) shows how the IV behavior evolves in response to the increase of T. At $T = 32$ mK, the subthreshold dV/dI drops substantially to ~10 MΩ, nearly one-tenth of that measured at 28 mK, even though a softer nonlinearity is retained.

The measured current rises rapidly around $V = 0.15$ mV. The nonlinear IV diminishes upon reaching $T \geqslant T_{c2}$. The recovery of the linear behavior is consistent with previous reports [11,12,15] interpreted as the onset of an isotropic liquid. Note that the linear behavior should not be confused with a metal since the differential resistance remains approximately 2MΩ well beyond h/e^2. Viscous flow in strongly correlated liquids is a likely candidate, and relevant theoretical work can be found in Ref. [39]. It is worth noting that the differential resistance, which measures the dynamical response, acquires approximately the same value for all three temperatures when the current drive is beyond 25 pA. The value of the differential resistance at this point agrees with the resistance under a thermal effect above 40 mK shown in Fig. 3(b). It therefore indicates that increasing the electric field results in similar changes to the electron states, even though it does not produce a clear discontinuity as observed in the thermally driven case.

Based on the results shown in both Figs. 3 and 4, it is clear that the discontinuity at T_{c1} separates a strong and a weak insulator. Both insulators are different from the unpinned situation above T_{c2}. Therefore, an intermediate state between T_{c1} and T_{c2} is supported. Nevertheless, the relevance to the theories on classical melting is yet to be confirmed because transitions involving hexatics [4–7,9], stripes/bubbles, and microemulsions [8] are expected to be second order.

A parallelism appears between the thermal and electric effects. There is a critical excitation where a threshold of current is triggered. Meanwhile, there is second critical excitation at a higher value above which the system attains the same dynamic response of an isotropic liquid, independent of T. The intermediate state is shown as the shaded region in Fig. 4(c).

The dc-IV response is drastically altered if the carrier density is above $p_c \sim 4.6 \times 10^9$ cm^{-2}. The dc-IV behavior obtained at similar T shown in Fig. 4(d) is for 5×10^9 cm^{-2}, which is just slightly above p_c. Threshold behavior diminishes completely and the differential resistance plummets to 1/20 000 of that for 3×10^9 cm^{-2} [Fig. 4(a)]. The inset is the same plot shown on the same scales of Fig. 4(c), which indicates a remarkable suppression of the resistance across p_c. Therefore, it provides further support to the critical behavior shown in Fig. 2(a) as an indication of a phase transition driven by increasing interaction near a critical point of $r_s \sim 40$.

The key findings of this study in terms of the discontinuity in the thermal effect and the critical behavior are absent in previous studies [11,15]. We offer two possible explanations. (i) The signal excitation used in previous studies is beyond the critical electric field, which is exceedingly small. (ii) T_{c1} (T_{c2}) is approximately 1/4 (1/3) of the classical melting point $E_c/127$, which cannot be accounted for by quantum fluctuations alone [30]. The suppression of T_c by disorder has been recognized [9,31], which could render the T_c beyond experimental reach.

The work at Wayne State University is supported by NSF under Grant No. DMR-1410302. The work at Princeton University was funded by the Gordon and Betty Moore Foundation through the EPiQS initiative Grant No. GBMF4420, and by the National Science Foundation MRSEC Grant No. DMR 1420541.

[1] E. Wigner, Phys. Rev. **46**, 1002 (1934).
[2] N. D. Mermin, Phys. Rev. **176**, 250 (1968).
[3] J. M. Kosterlitz, J. Phys. C **7**, 1046 (1974).
[4] B. I. Halperin and D. R. Nelson, Phys. Rev. Lett. **41**, 121 (1978).
[5] D. R. Nelson and B. I. Halperin, Phys. Rev. B **19**, 2457 (1979).
[6] D. R. Nelson and B. I. Halperin, Phys. Rev. B **21**, 5312 (1980).
[7] A. P. Young, Phys. Rev. B **19**, 1855 (1979).
[8] B. Spivak and S. A. Kivelson, Phys. Rev. B **70**, 155114 (2004).
[9] B. K. Clark, M. Casula, and D. M. Ceperley, Phys. Rev. Lett. **103**, 055701 (2009).
[10] H. W. Jiang, H. L. Stormer, D. C. Tsui, L. N. Pfeiffer, and K. W. West, Phys. Rev. B **44**, 8107 (1991).
[11] V. J. Goldman, M. Santos, M. Shayegan, and J. E. Cunningham, Phys. Rev. Lett. **65**, 2189 (1990).
[12] F. I. B. Williams, P. A. Wright, R. G. Clark, E. Y. Andrei, G. Deville, D. C. Glattli, O. Probst, B. Etienne, C. Dorin, C. T. Foxon, and J. J. Harris, Phys. Rev. Lett. **66**, 3285 (1991).
[13] S. V. Kravchenko, J. A. A. J. Perenboom, and V. M. Pudalov, Phys. Rev. B **44**, 13513 (1991).
[14] V. M. Pudalov, M. D'Iorio, S. V. Kravchenko, and J. W. Campbell, Phys. Rev. Lett. **70**, 1866 (1993).
[15] J. Yoon, C. C. Li, D. Shahar, D. C. Tsui, and M. Shayegan, Phys. Rev. Lett. **82**, 1744 (1999).
[16] P. Brussarski, S. Li, S. Kravchenko, A. Shashkin, and M. Sarachik, Nat. Commun. **9**, 3803 (2018).
[17] E. Y. Andrei, G. Deville, D. C. Glattli, F. I. B. Williams, E. Paris, and B. Etienne, Phys. Rev. Lett. **60**, 2765 (1988).
[18] Y. P. Chen, G. Sambandamurthy, Z. Wang, R. Lewis, L. Engel, D. Tsui, P. Ye, L. Pfeiffer, and K. West, Nat. Phys. **2**, 452 (2006).
[19] J. Jang, B. M. Hunt, L. N. Pfeiffer, K. W. West, and R. C. Ashoori, Nat. Phys. **13**, 340 (2017).
[20] P. W. Anderson, Phys. Rev. **109**, 1492 (1958).
[21] D. M. Ceperley and B. J. Alder, Phys. Rev. Lett. **45**, 566 (1980).
[22] T. M. Lu, Z. F. Li, D. C. Tsui, M. J. Manfra, L. N. Pfeiffer, and K. W. West, Appl. Phys. Lett. **92**, 012109 (2008).
[23] H. Zhu, K. Lai, D. Tsui, S. Bayrakci, N. Ong, M. Manfra, L. Pfeiffer, and K. West, Solid State Commun. **141**, 510 (2007).
[24] S. V. Kravchenko, G. V. Kravchenko, J. E. Furneaux, V. M. Pudalov, and M. D'Iorio, Phys. Rev. B **50**, 8039 (1994).
[25] N. Mott, J. Non-Cryst. Solids **1**, 1 (1968).
[26] B. I. Shklovskii and A. L. Efros, *Electronic Properties of Doped Semiconductors* (Springer Science & Business Media, Berlin, 2013), Vol. 45.
[27] K. J. Strandburg, Rev. Mod. Phys. **61**, 747 (1989).
[28] H. Noh, M. P. Lilly, D. C. Tsui, J. A. Simmons, L. N. Pfeiffer, and K. W. West, Phys. Rev. B **68**, 241308(R) (2003).
[29] J. Huang, D. S. Novikov, D. C. Tsui, L. N. Pfeiffer, and K. W. West, Phys. Rev. B **74**, 201302(R) (2006).
[30] M. Imada and M. Takahashi, J. Phys. Soc. Jpn. **53**, 3770 (1984).
[31] T. Knighton, Z. Wu, J. Huang, A. Serafin, J. S. Xia, L. N. Pfeiffer, and K. W. West, Phys. Rev. B **97**, 085135 (2018).

[32] J. Huang, L. N. Pfeiffer, and K. W. West, Phys. Rev. B **85**, 041304(R) (2012).
[33] B. Spivak, S. V. Kravchenko, S. A. Kivelson, and X. P. A. Gao, Rev. Mod. Phys. **82**, 1743 (2010).
[34] B. E. Kane, L. N. Pfeiffer, and K. W. West, Appl. Phys. Lett. **67**, 1262 (1995).
[35] J. Huang, D. S. Novikov, D. C. Tsui, L. N. Pfeifer, and K. W. West, Int. J. Mod. Phys. B **21**, 1219 (2007).
[36] M. Y. Simmons, A. R. Hamilton, M. Pepper, E. H. Linfield, P. D. Rose, D. A. Ritchie, A. K. Savchenko, and T. G. Griffiths, Phys. Rev. Lett. **80**, 1292 (1998).
[37] E. Berg, M. S. Rudner, and S. A. Kivelson, Phys. Rev. B **85**, 035116 (2012).
[38] G. Grüner, Rev. Mod. Phys. **60**, 1129 (1988).
[39] A. V. Andreev, S. A. Kivelson, and B. Spivak, Phys. Rev. Lett. **106**, 256804 (2011).